

# ANALYSIS OF SUN GLARE ON ROUNDABOUTS WITH AERIAL LASER SCANNING DATA

Silvia María González-Collazo<sup>a\*</sup>, Jesús Balado<sup>a</sup>, Elena González<sup>a</sup>, Mario Soilán<sup>b</sup>

<sup>a</sup>Universidade de Vigo, CINTECX, GeoTECH Group. 36310 Vigo, Spain  
(silygonzalez, jbalado, elena)@uvigo.es

<sup>b</sup>Department of Cartographic and Terrain Engineering, University of Salamanca, Calle Hornos 9 Caleros 50, 05003, Ávila, Spain  
msoilan@usal.es

## Commission II, WG II/10

**KEY WORDS:** solar incidence, road geometry, safety, driver's bearing, ALS point clouds

### ABSTRACT:

Road geometry and sun glares play an important role concerning road safety. In this research, the direct sunlight in a roundabout sited in Ávila (Spain) is analysed using Aerial Laser Scanning (ALS) point clouds. First, the roundabout is divided in 8 sections, obtaining the driver bearing vectors of the roundabout. Entrances and exits driver bearing vectors of the roundabout are also considered. Then, sun rays are generated for a specific location of the roundabout and in a specific day and time. The incidence of the sun rays with the driver's vision angle is analysed based on human vision model. Finally, intersections of sun rays with obstacles are calculated utilizing ALS point clouds. ALS data is processed (removing outliers, reducing point density, and computing a Delaunay Triangulation) in order to obtain accurate intersection results with obstacles and optimise the computational time. The method was tested in a roundabout, considering different driver bearings, the slope of the road and the elevation of the terrain. The results show that sun glares are detected at any day and time of the year, therefore areas with risk of direct sun glare within the roundabout are identified. The sun ray's incidence in the vision angle of the driver is higher during winter solstice, and intersections with obstacles occur mainly during sunrise and sunset. In roundabout vector 7, during winter solstice there is direct sun glare for 7 hours 30 minutes, at the equinoxes for 6 hours 15 minutes and during summer solstice there is no direct sun glare.

## 1. INTRODUCTION

Road network is hugely used for transportation of people and goods. The use of the road network deals also with the occurrence of traffic accidents influenced by several reasons such as traffic density, weather conditions and road geometry. Intersections, roundabouts and slope changes are road geometry features which can influence on traffic accidents. (González-Gómez and Castro, 2019) visibility is a relevant factor regarding safety, particularly in intersections which are complex areas due to their visual obstructions. The conversion of an intersection to a roundabout reduce the number of accidents, (Daniels et al., 2010). However, roundabouts with several lanes have a high number of possibilities for lane changes which implies a higher probability of accidents, (Balado Frias et al., 2019). (Hels and Orozova-Bekkevold, 2007) concluded that roundabouts are less safe for cyclist than for vehicles.

Sunlight and its incidence on the road are two characteristics that have influence on road safety. In some cases, the driver is blinded by the sunlight. Consequently, traffic accidents can increase, (Pegin and Sitnichuk, 2017). (Mitra, 2014; Sun et al., 2018) exposed that sun glare contributes to collision occurrence, especially at road intersections.

Aerial Laser Scanning (ALS) point clouds have been utilized in several studies. Road geometry is one of the features provided by road point clouds, which can be extracted from ALS data, (Widyaningrum et al., 2020). Having defined the road geometry,

it is possible to study how the geometry influence the road safety or the road visibility. ALS data is also used to study the elevations of the terrain. (Iglesias et al., 2016) concluded that ALS data is more accurate to analyse distant obstacles than MLS data.

The aim of this work is to evaluate safety conditions on roundabouts, considering the incidence of the Sun and the driver bearing vectors. To analyse the sun incidence, the azimuth and solar altitude are calculated for a given location and time. Roundabout geometry and the driver bearing vectors are taken manually from ALS point clouds. Then, the orientation of the sun rays is compared with the driver bearing vectors. Intersections with obstacles are searched using ALS data. For this purpose, it is necessary to process the point clouds (to remove outliers, reduce point density and triangulate them).

The rest of this paper is organized as follows. Section 2 presents the proposed method. The results are shown and analysed in Section 3. Section 4 concludes this work.

## 2. METHOD

The proposed method follows the subsequent stages, (Figure 1). First sun rays are calculated based on the solar angles (azimuth  $\beta$  and solar altitude  $\alpha$ ). Then, the incidence of sun rays in the driver's vision field is studied and finally, intersections of sun rays with obstacles are calculated.

\* Corresponding author

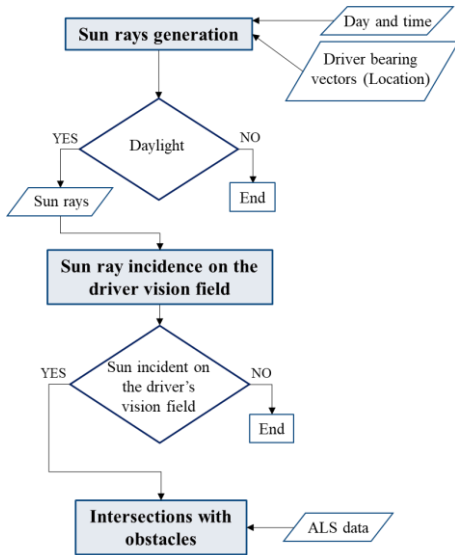


Figure 1. Workflow

## 2.1 Sun ray generation

Sun rays are calculated in order to analyse how the sunlight falls on the road. First, the latitude  $\gamma$  and longitude  $\varphi$  of each studied location are defined. Although a roundabout can be divided in an infinite number of ways to select and analyse the positions, in this study, eight locations within the roundabout are considered sufficient. Each change of section implies a bearing change of  $45^\circ$ . The vision angle is of  $120^\circ$ , therefore, this angle is covered. In addition to the locations within the roundabout, another location is added for each entry and exit lane. Locations and driver bearing vectors are generated manually based on the direction of driving.

The sun position is determined for a set of angles, (Figure 2):

- Declination angle  $\delta$ ; it is defined as the angle formed between the ecliptic plane and the equatorial plane.
- The hour angle  $\omega$ ; it represents the angular displacement of the Sun.
- Solar altitude  $\alpha$ ; it is defined as the elevation of the Sun with respect to the horizon.
- Azimuth angle  $\beta$ ; it is the angle formed by the south direction with the horizontal projection of the straight line connecting the position of the Sun with the observation point. Angles between south and northeast are negative and angles between south and northwest are positive.

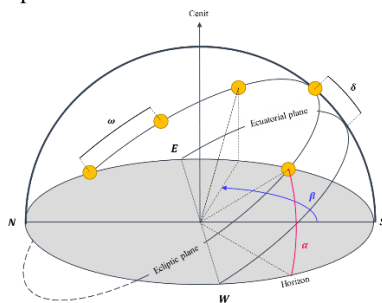


Figure 2. Solar angles: Declination  $\delta$ , hour angle  $\omega$ , azimuth angle  $\beta$  and solar altitude  $\alpha$

Angles which define the sun position are defined by the Equations 1 to 4, (Soilán et al., 2018).

$$\delta = 23.45 \sin\left(360 * \frac{284 + N}{365}\right) \quad (1)$$

$$\omega = 15 * (\text{solar\_hour} - 12) \quad (2)$$

$$\alpha = \text{asin}(\sin(\delta) * \sin(\varphi) + \cos(\delta) * \cos(\varphi) * \cos(\omega)) \quad (3)$$

$$\beta = \text{asin}(\cos(\delta) * \sin(\omega) / \cos(\alpha)) \quad (4)$$

Each location of the roundabout is defined as  $L = (L_x, L_y, L_z) \rightarrow Nx3$ , where  $N$  is the number of points. Considering the driver's high,  $L_z$  is assumed to be the altitude of the road plus 1.1 meters considering the vehicle using the road is a car, (Iglesias et al., 2016). The value of  $L_z$  could be different in case of a truck, bus or other vehicle model. Therefore, sun rays are defined as  $\theta = (L_x, L_y, L_z, \alpha, \beta)$ . Intersections of sun rays with obstacles are calculated utilising ALS point clouds.

## 2.2 Sun ray incidence on the driver vision field

The Sun has direct impact on the driver if sun rays are incident on the driver's vision field. Driver's vision field is defined by two planes, a horizontal plane and a vertical plane, (Figure 3a,b). The horizontal plane is defined by an angle between  $60^\circ$  and  $-60^\circ$  and the vertical plane is defined by an angle between  $50^\circ$  and  $-70^\circ$ , (Tara et al., 2020).

The sun rays incidence on the driver's vision field is analysed regarding the solar altitude  $\alpha$  and the azimuth angle  $\beta$ . The azimuth angle  $\beta$  is measured with respect to the south, however the driver bearing vector can be oriented in different directions regarding the cardinal axes (north, south, east, west, north-west, north-east, south-west and south-east). Therefore, the azimuth angle  $\beta$  is compared with the horizontal vision field considering the driver bearing angle regarding to the cardinal points, (Figure 3c). The solar altitude  $\alpha$  is compared with the vertical vision field. The slope of the road is considered, (Figure 3d). In the next stage it is analysed if any obstacles can occlude the direct incidence of the Sun.

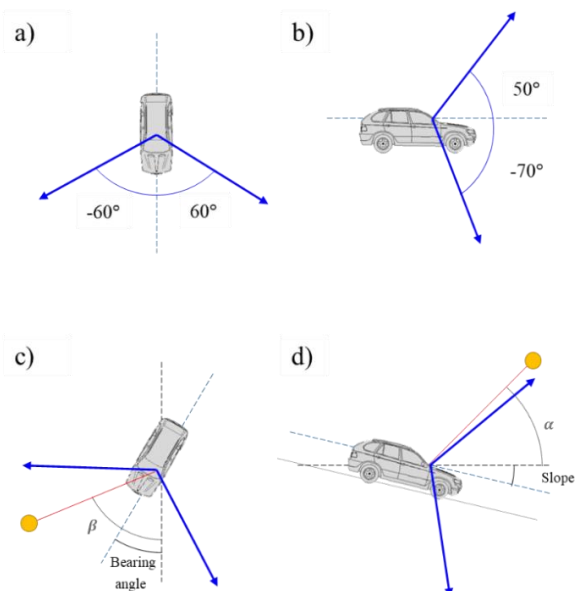


Figure 3. Driver's vision field: a) horizontal plane, b) vertical plane, c) analysis in the horizontal vision field d) analysis in the vertical vision field

### 2.3 Sun ray intersection with obstacles

Intersections of sun rays with obstacles are calculated to obtain the location and time at which the sunlight is occluded. In order to obtain intersections accurately, ALS point clouds,  $A = (A_x, A_y, A_z) \rightarrow Nx3$  where  $N$  is the number of points, are filtered and triangulated, (Figure 4). First, a Statistical Remove Outliers (SOR) filter, (Abdelazeem et al., 2021), is applied to eliminate noisy points which do not belong to the terrain. Then a point density reduction is applied and finally ALS point clouds are converted into a triangular mesh with the Delaunay Triangulation algorithm, (Dinas and Bañón, 2014). In this case it is not necessary to have a high level of detail. Obtaining the envelope of the terrain will be enough.

Intersections of the sun rays with obstacles are calculated, considering the location of the driver and the orientation of the sun rays. The mid-point of each driver bearing vector is chosen as the point of reference where the sun rays have incidence. Then, intersections of the sun rays  $\theta = (L_x, L_y, L_z, \alpha, \beta)$  with the triangular mesh are computed.

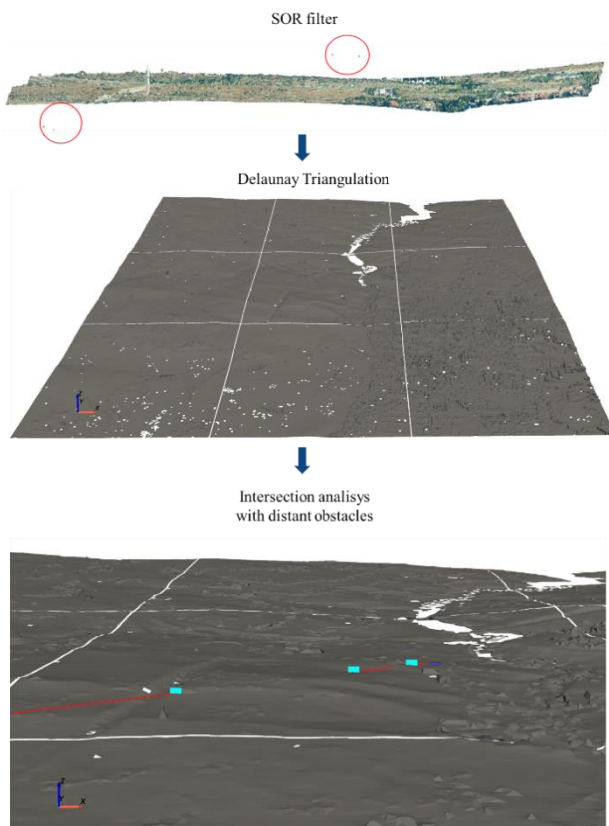


Figure 4. Workflow: Sun rays intersection with obstacles

## 3. EXPERIMENTS

### 3.1 Data

A roundabout sited in Ávila (Spain), with latitude 40.7° N and longitude 4.7° W, was selected as case study. ALS point clouds of this area were used to perform the proposed method. The ALS data were obtained from the Spanish National Geographic Information Centre (CNIG), considering 2 km as maximum distance to the roundabout. The Spanish ALS point cloud

database is organized in grids of 2x2 km, therefore, in this analysis 9 grids were considered with about 7,500,000 points grid, (Figure 5).



Figure 5. ALS point clouds. The blue square indicates the location of the roundabout

### 3.2 Parameters

ALS point cloud processing was done following the next stages: SOR filter, point density reduction and Delaunay Triangulation. Parameters used to perform these processes are shown in Table 1. The voxel size used for point density reduction decreases the number of points without losing significant detail of the terrain profile, allowing the computation time of subsequent steps to be reduced. With the size of the radius to perform the Delaunay triangulation, the triangulated terrain surface is obtained sufficiently detailed.

Operation	Parameters	
SOR Filter	No. neighbors = 20	Standard deviation = 5
Point density reduction	Voxel size = 20 cm	
Delaunay Triangulation	$\rho = 15$	

Table 1. Workflow parameters

### 3.3 Results

The proposed method was applied in the roundabout considering the driver bearing vectors of the 8 sections of the roundabout itself (R1 to R8), the driver bearing vectors of the 3 entrances (I1, I2, I3) and the driver bearing vectors of the 3 exits (O1, O2, O3) during each season (summer solstice, equinoxes and winter solstice), although it can be applied to any day of the year. Each bearing vector is defined by its orientation regarding the cardinal points, (Figure 6). In general, and due to the sun trajectory (sunrise in the east and pass through the south to sunset in the west), vectors oriented to the south are more affected by the direct sunlight.

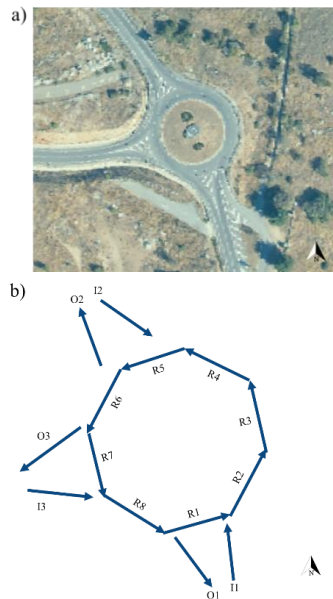


Figure 6. (a) Top view of the case study and (b) bearing vectors

Figure 7 shows the driver's vision in the horizontal plane (blue arrows) during each season, referring to the vector 5 of the roundabout. The number of hours where sun rays have incidence on the driver's vision in the horizontal plane increase from winter solstice to summer solstice (passing through the spring equinox). Solar altitude also increases, therefore sun rays are no longer incident on the vertical plane of vision when it is reached a certain height. During summer solstice sun rays are not incident in several hours of daylight due to the high altitude of the Sun, although they are incident in numerous hours of daylight in the horizontal plane of vision.

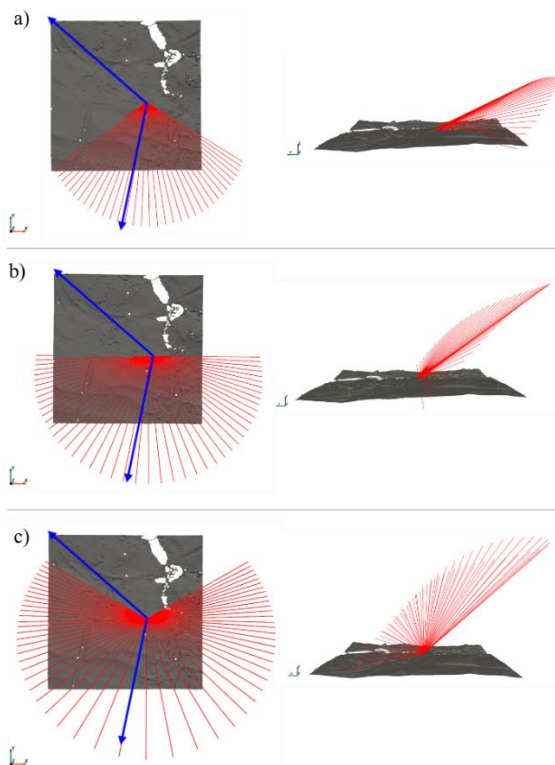


Figure 7. Sun rays during daylight (red lines) represented in the 2x2 km roundabout grid for a) winter solstice, b) equinoxes, c) summer solstice. river's vision field in the horizontal plane is indicated with blue arrows (referring to vector 5).

Intersections with obstacles were mainly encountered during sunrise and sunset. The terrain model had low altitudes and few altitude changes. Sun ray's incidence on the driver's vision field and intersections with obstacles were studied during daylight in each season. Figure 8 show intersections with obstacles in a specific roundabout vector, which occurred during the sunrise and the sunset in the winter solstice and in the equinoxes, and only during the sunset in the summer solstice.

Figure 9, Figure 10 and Figure 11 show the obtained results in each of the bearing vectors for the different seasons during daylight. In each vector is represented the solar hour at which the Sun had or not direct incidence in the driver's vision field and the solar hours at which the Sun was occluded by obstacles.

During winter solstice and equinoxes, the Sun had almost no incidence on the driver's vision field in roundabout vectors, entrances and exits which were oriented to the north. However, during summer solstice, the Sun had more incidence in these vectors due to the sun trajectory. The major incidence of sun rays on the driver's vision field occurred in south-facing vectors, although during summer solstice the sun ray's incidence was reduced due to the high solar altitude. Between 9:15 and 14:45 the Sun had not incidence in no location of the roundabout during summer solstice due to the high solar altitude  $\alpha$ . Sun rays had incidence at later daylight hours when vectors were oriented to the west. Roundabout vectors oriented to the east had sun ray's incidence at earlier daylight hours.

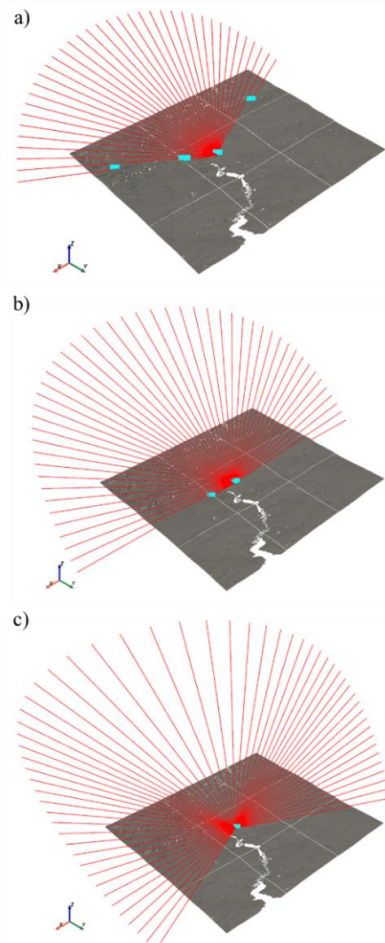


Figure 8. Sun ray intersections with obstacles in the roundabout vector 7 during daylight. Sun rays are represented by red lines and intersections are indicated with cyan points: a) winter solstice, b) equinoxes, c) summer solstice

Analysing driver bearing vectors, sun rays had incidence in the earlier hours of daylight in roundabout vector 1 and 2, oriented to north-east. In these locations, the more oriented to the east the more incidence of the sun rays at earlier hours of the daylight. Also the number of hours where the sun rays had incidence on the driver’s vision field increased from winter solstice to summer solstice. Similarly occurred in vectors oriented to south-east (roundabout vector 7 and 8, entrance 2 and 3, and exit 1), although, in these locations the more oriented to the east the earlier the Sun ceased to have incidence on the driver’s vision field. The number of hours where the Sun had incidence on the driver vision field is maximum during equinoxes. Results in north-west faced vectors (roundabout vector 3 and 4, entrance 1 and exit 2) and in vectors oriented to south-west (roundabout vector 5 and 6 and exit 3) are equivalent to the previous locations. However, the sun rays had incidence in the later hours of the daylight. In north-west face vectors, the more oriented to the west the higher number of hours where the Sun had incidence on the driver’s vision field. Also in north-west vectors the solar incidence increase from winter to summer solstice. In south-west vectors, the more oriented to the west the later the sun rays started to have incidence on the driver’s vision field.

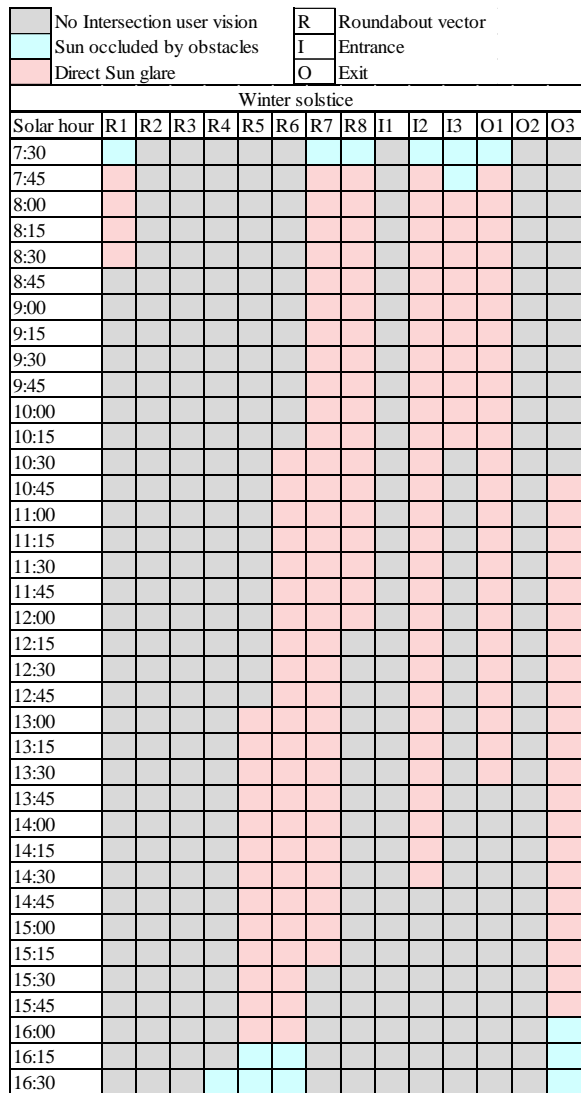


Figure 9. Sun rays incidence and intersections during winter solstice

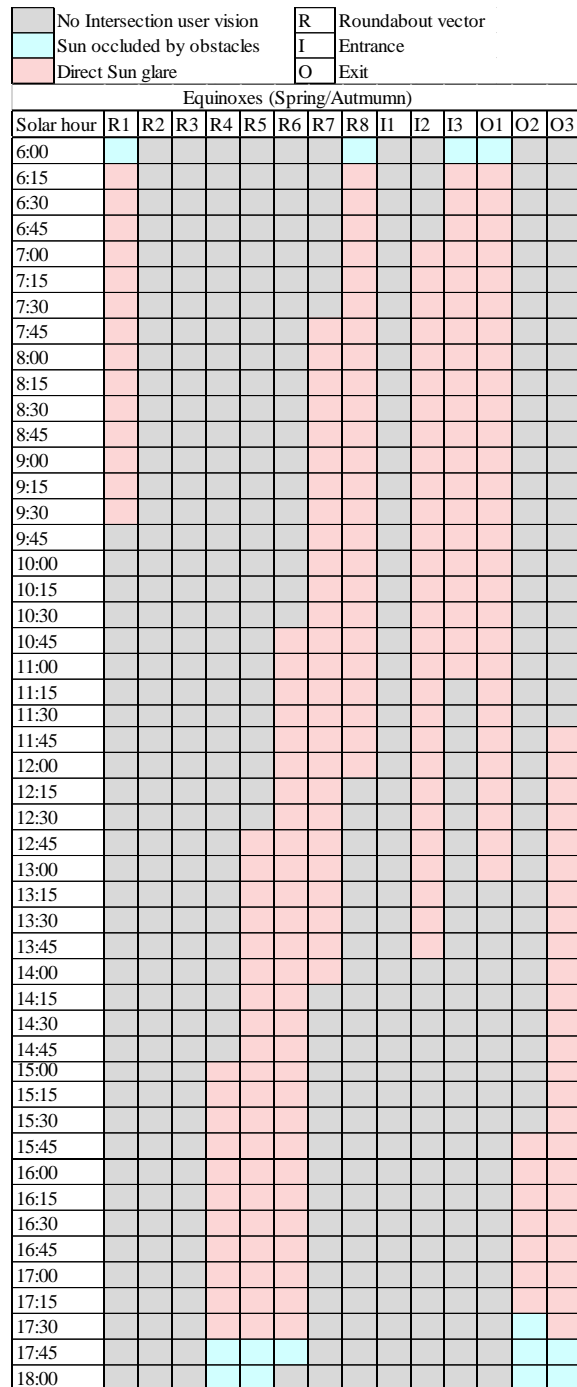


Figure 10. Sun rays incidence and intersections during equinoxes

		R	Roundabout vector												
		I	Entrance												
		O	Exit												
		Summer solstice													
Solar hour		R1	R2	R3	R4	R5	R6	R7	R8	I1	I2	I3	O1	O2	O3
4:45															
5:00															
5:15															
5:30															
5:45															
6:00															
6:15															
6:30															
6:45															
7:00															
7:15															
7:30															
7:45															
8:00															
8:15															
8:30															
8:45															
9:00															
9:15															
9:30															
9:45															
10:00															
10:15															
10:30															
10:45															
11:00															
11:15															
11:30															
11:45															
12:00															
12:15															
12:30															
12:45															
13:00															
13:15															
13:30															
13:45															
14:00															
14:15															
14:30															
14:45															
15:00															
15:15															
15:30															
15:45															
16:00															
16:15															
16:30															
16:45															
17:00															
17:15															
17:30															
17:45															
18:00															
18:15															
18:30															
18:45															
19:00															
19:15															

Figure 11. Sun rays incidence and intersections during summer solstice

All experiments were executed on Intel® Core™ i7 CPU 3.4GHz with 16GB RAM using Python. The total time processing considering one season and analysing all driver bearing vector was 6' 48". The time processing detail is shown in Table 2.

Operation	Time processing	Number of executions
Data reading and latitude and longitude calculation	1'	One execution
Sun position and sun trajectory calculation	1'	Executed for each season
Filtering and triangulation of ALS point clouds	2' 12"	One execution
Calculating intersections	12"	Executed for each driver bearing vector

Table 2. Time processing detail

### 3.4 Analysis and discussion

An analysis was performed by selecting a specific hour. Sun ray's incidence was studied in every driver bearing vectors and for different seasons. The solar altitude  $\alpha$  increases from the winter solstice through the autumnal equinox to the summer solstice. During winter solstice occurred several intersections (Figure 12a) while in equinoxes and in summer solstice did not occur intersections with the terrain due to the solar altitude is high and the elevation of the terrain is low, (Figure 12b).

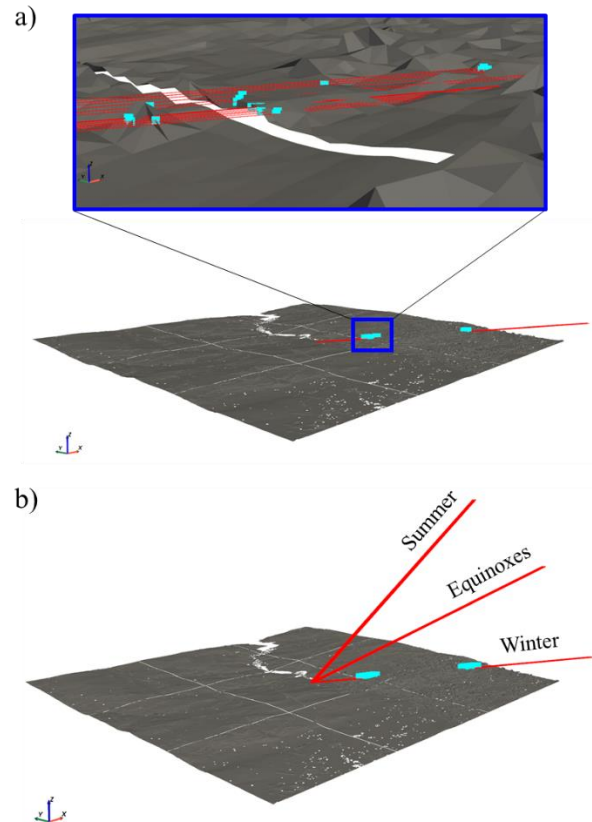


Figure 12. Sun ray intersections with obstacles in the roundabout at 7:30. Sun rays are represented by red lines and intersections are indicated with cyan points: a) winter solstice with zoom in intersections, b) summer solstice, equinoxes and winter solstice

Results demonstrated that the incidence of sun rays in the driver's vision field depend largely on the driver's vector bearings and also on the day and hour of the year (azimuth  $\beta$  and solar altitude  $\alpha$ ). Intersections with obstacles depend on the altitude of the terrain and accordingly on the day and hour of the year.

All the experiments were analysed considering direct sunlight in sunny days. Clouds and other meteorological factors could

minimize the incidence of the sun rays; however, this is out of the scope of the work. Neither adverse weather conditions (rain, snow, fog) have been considered in the proposed method.

In this case of study, the roundabout is not surrounded by near obstacles which can occlude the Sun (vegetation, buildings, road elements). ALS data is sufficient to analyse intersections with obstacles, however, given the limitations in acquiring vertical elements, another data source should be used to detect near obstacles and obtain a more accurate triangulation.

#### 4. CONCLUSIONS

Find the areas where sun rays have incidence on the driver's vision field is a crucial feature in order to prevent accidents and propose measurements to reduce them. In this research is presented a method to detect sun glares in roundabouts. It is applied at days and times where the direct sunlight has incidence on the driver's vision field and has into consideration locations where sun rays are occluded by the altitude of the terrain. The method is applicable to any day and time of the year and for any location at the roundabout, considering the driver bearing, the road geometry and the sun position.

The experimental results, on a roundabout sited in Ávila (Spain), show that the incidence of the sun rays in the driver's vision field are closely related with the bearing of the driver. Due to the sun trajectory (rises in the east and sets in the west) the orientation more exposed to sunlight is the south. However, during summer solstice there were some exceptions because the Sun rises in the north-east and sets in the north-west. The azimuth angle and the solar altitude are also relevant features. Low altitudes imply a greater incidence of the sun rays in the driver's vision field and also greater number of intersections with obstacles. Winter solstice is the season where the Sun is at its lowest position and therefore the season where the sun rays had more intersections with obstacles. However, summer solstice is the season where the Sun is at its highest position and therefore the season where sun rays had the least incidence on the driver's vision field and where there were the fewest intersections with obstacles. Intersections occurred during sunrise and sunset, because the solar altitude is low and the terrain had low altitudes.

The method can be applied in high accident areas to assist decision-making. Illuminated signs could be installed to warn of reduced visibility at specific times of the day, and the algorithm could be used in accident blackspots or road accidents. In addition, notifications could be implemented in navigation systems to warn of potential sun glares.

Future work will focus on extending the test on different types of intersections (direction changes on road, intersections). Cloudy days and adverse weather conditions (rain, fog, snow) will also be considered, reevaluating the incidence of the sun and considering the reflections of sun rays. Other types of data (Terrestrial Laser Scanning or Mobile Laser Scanning) may be used to obtain more accurate information, especially of obstacles in the vicinity of the road. In addition, other models of visibility and solar incidence in different geometries will be investigated.

#### ACKNOWLEDGEMENTS

This research was funded by the Xunta de Galicia, grant numbers ED481B-2019-061 and ED431C 2020/01, and by the Spanish Ministry of Science and Innovation, grant numbers PID2019-105221RB-C43/AEI/10.13039/501100011033, TIN2016-77158-C4-2-R and FJC2018-035550-I funded by MCIN/AIE/

10.13039/501100011033. This paper was carried out in the framework of the InfraROB project (Maintaining integrity, performance and safety of the road infrastructure through autonomous robotized solutions and modularization), which has received funding from the European Union's Horizon 2020 research and innovation programme under grant agreement no. 955337. It reflects only the authors' views. Neither the European Climate, Infrastructure, and Environment Executive Agency (CINEA) nor the European Commission is in any way responsible for any use that may be made of the information it contains.

#### REFERENCES

- Abdelazeem, M., Elamin, A., Afifi, A., El-Rabbany, A., 2021. Multi-sensor point cloud data fusion for precise 3D mapping. *Egypt. J. Remote Sens. Sp. Sci.* <https://doi.org/https://doi.org/10.1016/j.ejrs.2021.06.002>
- Balado Frias, J., Díaz Vilariño, L., Arias, P., Novo, A., 2019. A safety analysis of roundabouts and turbo roundabouts based on Petri nets. *Traffic Inj. Prev.* 20, 1–6. <https://doi.org/10.1080/15389588.2019.1594208>
- Daniels, S., Brijs, T., Nuyts, E., Wets, G., 2010. Explaining variation in safety performance of roundabouts. *Accid. Anal. Prev.* 42, 393–402. <https://doi.org/https://doi.org/10.1016/j.aap.2009.08.019>
- Dinas, S., Bañón, J., 2014. A review on Delaunay Triangulation with application on computer vision. *IJCSE - Int. J. Comput. Sci. Eng.* 3, 9–18.
- González-Gómez, K., Castro, M., 2019. Evaluating Pedestrians' Safety on Urban Intersections: A Visibility Analysis. *Sustainability* 11. <https://doi.org/10.3390/su11236630>
- Hels, T., Orozova-Bekkevold, I., 2007. The effect of roundabout design features on cyclist accident rate. *Accid. Anal. Prev.* 39, 300–307. <https://doi.org/https://doi.org/10.1016/j.aap.2006.07.008>
- Iglesias, Ó., Díaz-Vilariño, L., González-Jorge, H., Lorenzo, H., 2016. Interurban visibility diagnosis from point clouds. *Eur. J. Remote Sens.* 49, 673–690. <https://doi.org/10.5721/EuJRS20164935>
- Mitra, S., 2014. Sun glare and road safety: An empirical investigation of intersection crashes. *Saf. Sci.* 70, 246–254. <https://doi.org/https://doi.org/10.1016/j.ssci.2014.06.005>
- Pegin, P., Sitnichuk, E., 2017. The Effect of Sun Glare: Concept, Characteristics, Classification. *Transp. Res. Procedia* 20, 474–479. <https://doi.org/10.1016/j.trpro.2017.01.077>
- Soilán, M., Riveiro, B., Liñares, P., Padín-Beltrán, M., 2018. Automatic parametrization and shadow analysis of roofs in urban areas from ALS point clouds with solar energy purposes. *ISPRS Int. J. Geo-Information* 7, 1–14. <https://doi.org/10.3390/ijgi7080301>
- Sun, D., El-Basyouny, K., Kwon, T.J., 2018. Sun Glare: Network Characterization and Safety Effects. *Transp. Res. Rec.* 2672, 79–92. <https://doi.org/10.1177/0361198118784143>
- Tara, A., Lawson, G., Renata, A., 2020. Measuring magnitude of change by high-rise buildings in visual amenity conflicts in

Brisbane. *Landsc. Urban Plan.* 205.  
<https://doi.org/10.1016/j.landurbplan.2020.103930>

Widyaningrum, E., Peters, R.Y., Lindenberg, R.C., 2020.  
Building outline extraction from ALS point clouds using medial  
axis transform descriptors. *Pattern Recognit.* 106, 107447.  
<https://doi.org/https://doi.org/10.1016/j.patcog.2020.107447>